Correlation between nodular morphology and fracture properties of cured epoxy resins

Jovan Mijović
Polytechnic Institute of New York, Department of Chemical Engineering, 333 Jay St., Brooklyn, NY 11201, USA
and J. A. Koutsky
University of Wisconsin – Madison, Chemical Engineering Department, Madison, Wisc. 53706, USA
(Received 27 December 1978; revised 19 March 1979)

Various bulk epoxy resin formulations, based on diglycidyl ether of bisphenol A (DGEBA) and cured with diethylene triamine (DETA) were studied. Methods of linear elastic fracture mechanics were employed and all systems were characterized by the corresponding values of the critical strain energy release rate for crack initiation and crack arrest. Fracture morphology was studied by scanning electron microscopy and transmission electron microscopy of carbon–platinum surface replicas. An apparent correlation between morphology and ultimate mechanical properties has been found. All fracture surfaces are shown to be characterized by distinct nodular morphology. Nodules, ranging in size from 15–45 nm, represent the sites of higher crosslink density in an inhomogeneous network structure. Fracture surfaces were further characterized by three crack propagation zones. A smooth, brittle fracture zone was preceded and followed by crack initiation and crack arrest zones, respectively. An apparent plastic flow was confined to the initiation and arrest regions. No crazing phenomenon was seen in the initiation zone; instead a step-like fracture was observed, typified by the 'flow' of internodular matrix during step formation. Local plastic deformation in the initiation zone and the corresponding value of critical strain energy release rate, G_{Ic}, were correlated with the nodular morphology. The size of nodules was found to vary with the curing agent concentration, thus allowing us to establish a fundamental correlation between the nodular morphology and the ultimate mechanical properties of epoxy resins.

INTRODUCTION

Morphology

Initial efforts to understand the morphology of thermosets date back to the mid-thirties when de Boer[1] showed that the tensile strength of several thermosetting resins was significantly lower than the theoretical value calculated assuming a formation of C–C bonds throughout the entire mass of a resin. According to his calculations, even if the irregular 'blocks' (apparently inhomogeneities in the resin structure, QEI) were assumed to be held together by secondary forces, the theoretical value of tensile strength was still approximately five times higher. An earlier theory[2,3] (Smekal's 'Lockerstellentheorie') suggested that the observed low values of tensile strength of metals were caused by the high concentration of stresses at structural defects. Smekal's theory had its unambiguous precursor in the classical study by Griffith[4], who showed that the rupture of an amorphous body (glass) does not take place simultaneously over the entire cross-section but starts from the accidental flaws.

Considering these findings, Houwink[5] pointed out that flaws or defects in thermosetting resins are not accidental but rather structural features of statistical nature. Due to steric factors, chemical reactions between the functional groups become impossible at certain positions in the resin, resulting in a formation of weak spots ('Lockerstellen').

Houwink's work was followed by a long period of time which was devoid of attempts to understand thermoset morphology, until an entirely different model of morphology of crosslinked polymers emerged from the analysis of Flory[6]. Assuming chemical equivalency of different functional groups and the absence of intramolecular reactions in polyfunctional condensations, Flory established conditions necessary for the formation of an infinite network. The end result would be a homogeneous structure represented by one giant molecule. It should be emphasized, however, that most of Flory's experimental results were obtained from polyesterification reactions which, with reactive groups spaced further apart, do not present an adequate model of highly crosslinked thermosetting resin structures. Nonetheless, the idea of lower molecular weight fractions being eventually attached to the 'indefinitely large structure' has appealed to many polymer scientists and thereafter all amorphous polymers have been commonly thought of as homogeneous infinite networks.

However, a growing demand for the understanding of thermoset morphology has been constantly initiating new research efforts and consequently, within the last two decades, more experimental evidence for the existence of inhomogeneities in thermoset morphology has been obtained[7–27]. The main body of evidence came from electron microscope studies, although conclusive results also emerged from differential thermal analysis, differential scanning calorimetry, dynamic mechanical measurements, and swelling experiments.

To summarize all these studies, it is generally agreed that the more highly crosslinked nodules, ranging in size from 6 nm to 10 μm, are surrounded by a lower molecular weight matrix. The actual mechanism of formation of nodules and the effect that they impart on the macroscopic properties

0032–3861/79/091095–13$02.00

of thermosets are areas of current research. Nevertheless, the inability to detect nodular structures by small-angle X-ray scattering and small-angle neutron scattering has initiated some antinodular arguments. Dušek *et al.*[28] (in a recent article entitled: 'Are cured epoxy resins inhomogenous?') showed apparent nodular structure in electron micrographs of plasma-etched fracture surfaces of various epoxy resins. However, these authors note that the existence of nodules on fracture surfaces of polystyrene (PS) and poly(methyl methacrylate) (PMMA) and the failure of small-angle X-ray scattering to distinguish between phases of different electron density, disagree with postulated inhomogeneous crosslinking. Thus, a stimulating controversy exists, and this study is intended to present another contribution toward clarification of the idea of inhomogeneities in thermoset morphology.

Linear elastic fracture mechanics

To correlate quantitatively the observed resin morphology to ultimate mechanical properties, a material property was sought which would most adequately characterize thermosetting resins. An extensive application of thermosets as adhesives and matrices in composites, dictates that the design criteria for these materials be based upon the reliability against brittle fracture. This is, indeed, the exact domain of methods developed relatively recently for linear elastic fracture mechanics (*LEFM*). The *LEFM* analysis, originally applied to glass and metals, was later successfully extended to various brittle thermosets, both in the form of bulk materials and as adhesives. Basic concepts of the theory of linear elastic fracture mechanics are discussed elsewhere[28–31]. An enormous interest for this type of study has been generated in aircraft and spacecraft industries since the reliability of thermosets (e.g. aluminium–epoxy adhesive joints) has been directly linked to their fracture energy (strain energy release rate). The critical value of strain energy release rate, at given loading rate and environmental conditions, represents a geometry-independent material property and as such is suitable for specifying the ultimate mechanical properties and requirements of structural materials.

The strain energy release rate, G, can be thought of as the energy required to extend a pre-existing crack an infinitesimal unit of area. A critical value of the strain energy release rate at which the crack extends in mode I is designated G_{Ic}. An expression for G_{Ic} is given by:

$$G_{Ic} = \frac{P_c^2}{2B}\left(\frac{\partial C}{\partial a}\right)_P \qquad (1)$$

where G_{Ic} (J/m^2 or lb/in.) = critical strain energy release rate: P_c (kgf or lb) = critical load; B(cm or in.) = specimen width, and $(\partial C/\partial a)_P$ = change of compliance with crack length at constant load.

Uniform double cantilever beam (*UDCB*) arrangements employed in early studies[32,33], represented an elaboration of Obreimoff's experiment[34] on the cleavage of mica, carried out in 1930.

In the mid-sixties, an ingenious development was reported[35,36]. A system was designed with a constant compliance change with crack length ($\partial C/\partial a$ = constant) by varying the height of the specimen along the crack propagation path. Contoured specimens of this type are referred to as tapered double cantilever beam (*TDCB*) specimens. This greatly simplifies the actual experimental determination of the critical strain energy release which becomes a function of the critical load only.

It can easily be shown that the expression for the critical strain energy release rate of bulk materials assumes the following form:

$$G_{Ic} = \frac{4m'}{EBB_n} P_c^2 \qquad (2)$$

where E (dyne/cm^2 or lb/in.^{2}) = elastic modulus; P_c (kgf or lb) = critical load; B (cm or in.) = specimen width; B_n (cm or in.) = specimen width in the crack propagation plane, and m' (cm^{-1} or in.$^{-1}$) = experimentally corrected value of m (a numerical constant which determines the shape of the tapered region). To calculate m' accurately, a set of compliance calibration measurements is performed as described elsewhere[36–38].

Fracture energies of bulk epoxy resins of DGEBA type, as obtained from the cleavage tests of TDCB specimens by several workers, are provided in *Table 1*.

EXPERIMENTAL

Chemical Systems

The chemical structure of epoxy resin and curing agent used in this work is presented in *Table 2*. The composition and cure schedule of various epoxy resin formulations are listed in *Table 3*.

Techniques

TDCB samples for fracture energy measurements and specimens for determination of tensile and bending moduli were cast in silicone rubber moulds. A Silastic E RTV rubber (Dow Corning) cured with 10 phr* of Silastic E curing agent for 24 h at room temperature, was used for the moulds.

All bulk specimen dimensions (cm) are given in *Figures 1–3*. The *TDCB* specimens were contoured in such a manner that the compliance changed linearly with the crack length. The expression for calculation of the fracture energy is given by equation (2).

Side grooves and grip holes were machined on all bulk specimens prior to testing. Each specimen was then slit to the tapered section with a jeweller's saw. A 'V'-shaped chevron was cut and an approximately 5 mm long precrack was tapped in with a single edge razor blade.

The Young's moduli of elasticity (tensile moduli) were obtained from the slope measurements of stress–strain diagrams. All epoxy formulations studied displayed linear σ–ϵ behaviour almost up to the fracture point.

Bending moduli of elasticity of epoxy beams were determined from the equation:

$$E = \frac{4PL^3}{Bh^3y} \qquad (3)$$

where E(dyne/cm^2 or lb/in.^{2}) = bending modulus of elasticity: P(kgf or lb) = applied load; L (cm or in.) = beam length; B(cm or in.) = beam thickness; h (cm or in.) = beam height; and y (cm or in.) = deflection.

Experimentally, load–deflection diagrams were obtained

* phr = parts per hundred parts of resin, by wt

Table 1 Fracture energies of bulk epoxy resins of the DGEBA type obtained from cleavage tests of tapered double cantilever beam specimens*

Reference	Epoxy resin	Curing agent	System characteristics	Reinforcement	Purpose of investigation	Approximate range of G_{Ici} values (lb/in.)	(J/m^2)
33	Epon 825	DETA	UDCB Specimens 10% DETA, cured 24 h at RT + post-cure at 240°F	–	Fracture surface work calculated	0.25	43
35	DER 332	TEPA (tetraethylene pentamine)	Various TEPA concentrations 1 h at 150°F + 5 h at various post-cure temperatures	–	G_c as a function of curing agent concentration and post-cure temperature	0.3–1.3	52–227
43	DER 332	HHPA (hexahydrophthalic anhydride)	Various HHPA concentrations + 2 phr of acceleration – 2, 4, 6-tri-dimethylamino methyl phenol, 5 h at various post-cure temperatures	–	G_c as a function of curing agent concentration and post-cure temperature	0.9–4.5	158–262
53	Epon 825	'D'	5% 'D' UDCB specimens	Various carboxy-terminated butadiene–acrylonitrile (CTBN) particles	Fracture surface work as a function of the type of CTBN particles	1.0	175
58	DER 332	HHPA	31.2 phr HHPA + 0.2 wt % BDMA (cat) 2 h at 90°C + 16 h at 120°C + 2 h at 150°C	–	G_{Ic} only reported	0.78	136
58	DER 332	m-PDA (*meta*-phenylene diamine)	13.7 phr m-PDA, 16–20 h at RT + 1 h at 66°C + 3 h at 149°C + 2 h at 160°C	–	G_{Ic} only reported	0.84	148
58	DER 332	NMA ('Nadic' methyl anhydride)	46.6 phr NMA + 0.8 wt % BDMA (cat) 2 h at 100°C + 2 h at 135°C + 2 h at 166°C	–	G_{Ic} only reported	0.38	67
59	Epikote 828	'Epikure NMA'	95 phr 'Epikure NMA' + 0.5 phr BDMA (cat), 4 h at 100°C + 3 h at 180°C, Instron crosshead speed = 0.4 mm/min. UDCB specimens	–	Fracture surface energy as a function of crack length and immersion in water	0.91	160
60	DER 332	Piperidine	5 phr piperidine, 16 h at 120°C	Carboxy-terminated butadiene–acrylonitrile (CTBN), 0–30 wt %	G_c as a function of curing agent concentration and adhesive thickness	0.69–21	121
61	DER 332	Piperidine	5 phr piperidine, 16 h at 120°C	15 wt % CTBN	G_c as a function of temperature	0.69–7.5	121–1312

* All values obtained with TDCB specimens in mode I testing at room temperature and a loading rate of 0.05 in/min, unless otherwise indicated

Table 2 Chemical structure of epoxy resin and curing agent

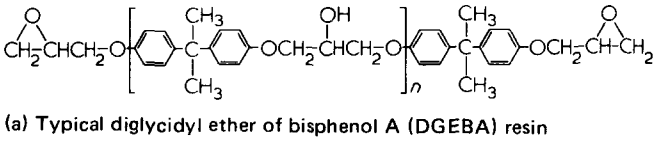

(a) Typical diglycidyl ether of bisphenol A (DGEBA) resin

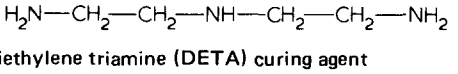

(b) diethylene triamine (DETA) curing agent

and values of bending moduli of elasticity calculated from the slope measurements.

All samples were kept at 72°F and 45% r.h. for at least 24 h prior to testing. An Ametek–Riehle Testing Equipment system was used for the fracture energy determination, tensile and bending moduli determination and compliance calibration. All tests were performed at a crosshead speed of 0.2 cm/min.

One-stage and two-stage carbon–platinum (C–Pt) replicas of all parts of fracture surfaces were made and studied by transmission electron microscopy. A CVC CVE-14 evaporator was used for C–Pt replication at pressures of less than 5×10^{-5} torr. The replica preparation method is described elsewhere[39]. A model HUS-4GB Hitachi evaporator operated at pressures of less than 10^{-5} torr was used for chromium and gold shadowing for scanning electron microscopy studies. A Cwikscan 100 scanning electron microscope and a JEOL 100B transmission electron microscope were used to investigate the fracture surfaces. Selective etching of fracture surfaces with acetone at room temperature was carried out to obtain more information about the fracture surface morphology.

RESULTS

Fracture mechanics tests

All fracture mechanics data are expressed in terms of the critical strain energy release rate (G_{Ic}) and it is appropriate to start this section by defining the meaning of this symbol clearly. Although the critical strain energy release rate is often referred to as a material property, it is necessary to

Table 3 Various epoxy formulations studied

Formulation or cure schedule no.	Composition	Variable	Cure schedule
1	Epon 825* + 8 phr DETA	Post-cure time	Components mixed at RT for 5 min and poured in silicone moulds; 24 h at RT + post-cure at 106°C
2	Epon 825 + 6–11 phr DETA	Curing agent concentration	Components mixed at RT for 5 min and poured in silicone moulds; 24 h at RT + 20 h at 120°C
3	Epon 825 + 8 phr DETA	Aggressive environment; 5 weeks in H_2O and C_2H_5OH	Components mixed at RT for 5 min and poured in silicone moulds; 24 h at RT + 20 h at 120°C
4	Epon 825 + 8 phr DETA	Cyclic exposure to −18°F for 9 h + 80°F and 90% r.h. for 15 h. Cycle was repeated from 1 to 7 days	Same as formulation 3

* Epon 825, Shell's liquid DGEBA resin, is a purified form of commercially available Epon 826

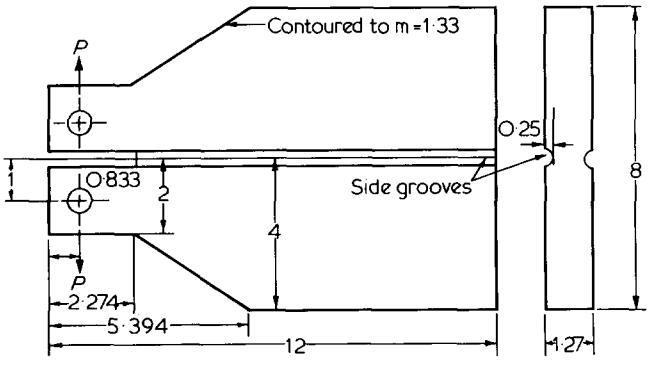

Figure 1 Tapered double cantilever beam (*TDCB*) specimen for mode I fracture testing of bulk specimens. All dimensions in *Figures 1, 2* and *3* in cm

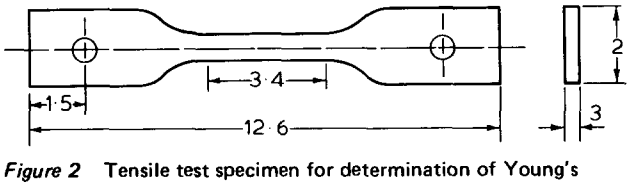

Figure 2 Tensile test specimen for determination of Young's modulus

realize its dependence upon the loading rate[40,41] temperature[35,42] and aggressive environment such as water or various solvents[43,44]. The often claimed advantage of critical strain energy release rate as a geometry-independent material property should be also approached with caution. Experimentally, a certain minimum specimen thickness exists, only beyond which G_{Ic} becomes truly geometry-independent under plane strain conditions[45]. Consequently, upon placing all of these restrictions on a G_{Ic} value, a 'true material property' label becomes something of a misnomer. Nevertheless, throughout this work we will refer to G_{Ic} as a material property but will always specify the above-mentioned restrictions.

Immediately upon the extension of the tapped-in precrack, samples were unloaded and then reloaded, until the critical load values for crack initiation (P_{ci}) and arrest (P_{ca}) were obtained. This procedure was repeated to obtain as many data points as possible. Only samples that produced at least two data points within the tapered section were taken into account for calculations. Three test specimens were run, and thus at least six data points were collected for each sample. Only unstable crack propagation was observed in all systems.

The effect of various post-cure times on the fracture energy of bulk epoxy resins was studied first. A formulation consisting of Epon 825/8 phr DETA was subjected to cure schedule 1 (*Table 3*). Fracture energies for crack initiation (G_{Ici}) and arrest (G_{Ica}) as a function of post-cure time are given in *Figure 4*. Higher values of G_{Ic} were observed within the first 20 h of post-cure. After approximately 20 h the scatter of data was reduced and the value of G_{Ic} became nearly constant. In addition, several samples of DER 332 (Dow's liquid DGEBA-type epoxy resin) were cast and subjected to cure schedule 1 (*Table 3*). Values of fracture energies of initiation and arrest for specimens post-cured between 0 and 5 h closely followed the pattern observed with Epon 825 resin (*Figure 4*). Also, the difference of $G_{Ici}-G_{Ica}$ becomes greater at longer post-cure times (*Figure 5*), indicating further embrittlement of the epoxy resin since the crack upon initiation travels for longer distances and eventually stops when the energy stored in the beams is sufficiently lowered.

Figure 6 shows the fracture energies for crack initiation and crack arrest as a function of curing agent concentration

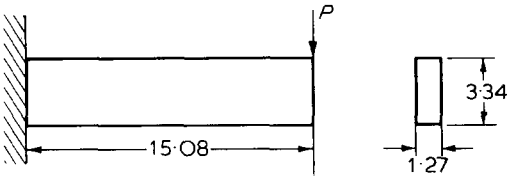

Figure 3 Specimen for determination of bending modulus

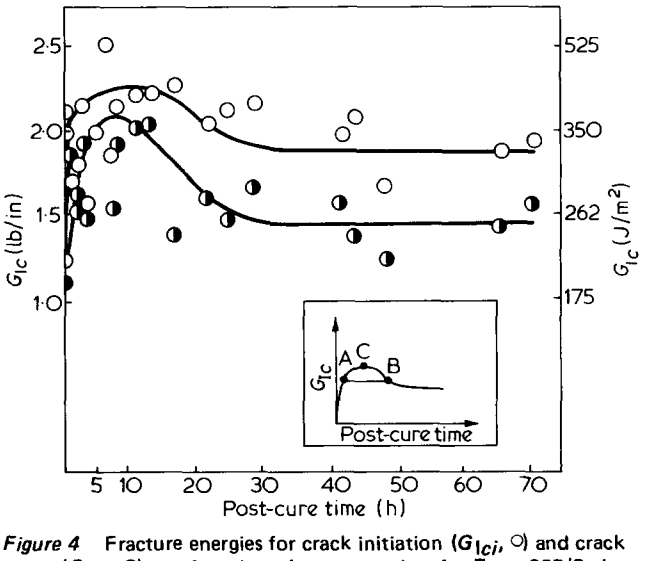

Figure 4 Fracture energies for crack initiation (G_{Ici}, ○) and crack arrest (G_{Ica}, ●) as a function of post-cure time for Epon 825/8 phr DETA system subjected to cure schedule 1 (*Table 3*)

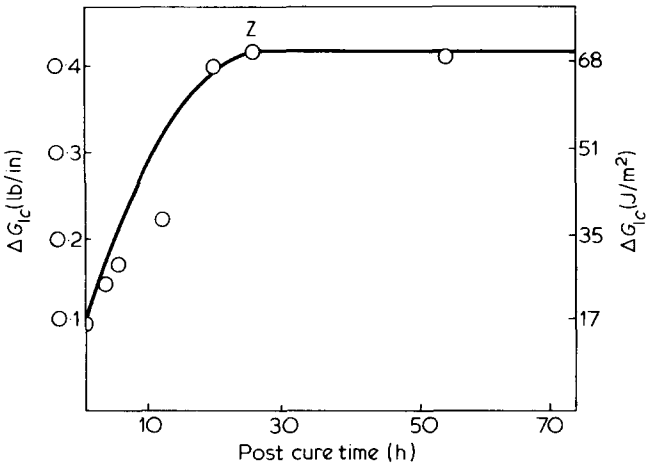

Figure 5 ΔG_{Ic} ($G_{Ici} - G_{Ica}$) as a function of post-cure time for Epon 825/8 phr DETA system subjected to cure schedule 1 (*Table 3*)

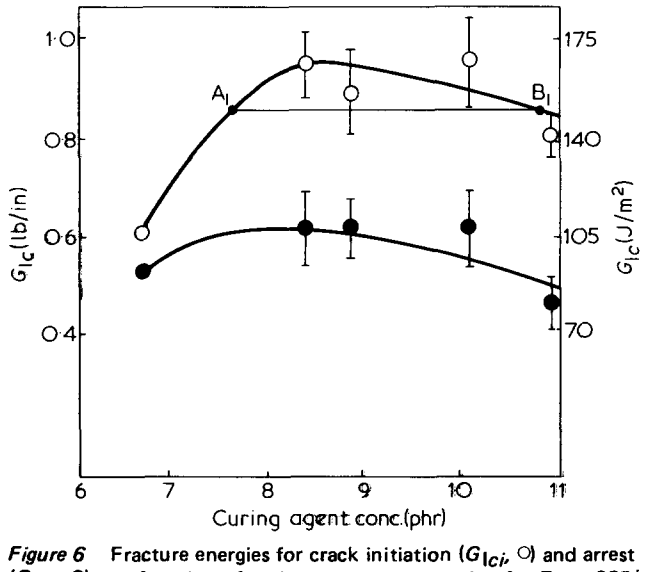

Figure 6 Fracture energies for crack initiation (G_{Ici}, ○) and arrest (G_{Ica}, ●) as a function of curing agent concentration for Epon 825/ various phr of DETA systems subjected to cure schedule 2 (Table 3)

for resin formulation 2 (*Table 3*). An initial increase in G_{Ic} was followed by a slight drop beyond the value of 8 phr of DETA. Also, the difference between fracture energies for crack initiation and crack arrest ($\Delta G_{Ic} = G_{Ici} - G_{Ica}$, *Figure 7*) is shown to increase with curing agent concentration. An abrupt increase in ΔG_{Ic} was noted up to approximately 8 phr of DETA; no apparent change was observed beyond that point. We again emphasize the similarity with the ΔG_{Ic} dependence on post-cure time (*Figure 5*). It appears that, in both cases, an asymptotic value of ΔG_{Ic} unambiguously indicates the point at which the ultimate brittleness of material is reached (at a given temperature, loading rate and environmental conditions) as a function of curing agent concentration and/or post-cure time.

In an attempt to study the effect of cyclic exposure to various environmental conditions onto fracture properties of an Epon 825/DETA system, samples were subjected to cure schedule 4 (*Table 3*) and cyclically exposed to an aggressive environment (see *Table 3*) from 1 to 7 days. Our goal was to determine the influence of hostile environment on fracture properties, find a correlation with morphological changes and establish a possible behavioural trend towards the prediction of long-term performance in service. However, only insignificant changes in the fracture energy values were observed (*Figure 8*). G_{Ici} and G_{Ica} values calculated from the experimental data, were similar to those of fully-cured specimens which, *except* for the cyclic exposure to the aggressive environment, were subjected to the same cure schedule.

Higher values of the critical strain energy release rate were obtained upon a 5 week exposure of precracked samples to water and alcohol. In *Table 4*, a direct comparison of the G_{Ic} values of samples unexposed and exposed to different

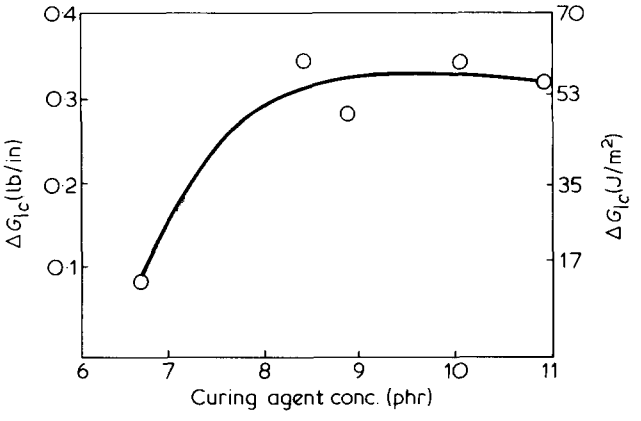

Figure 7 ΔG_{Ic} ($G_{Ici} - G_{Ica}$) as a function of curing agent concentration for Epon 825/various phr of DETA systems subjected to cure schedule 2 (*Table 3*)

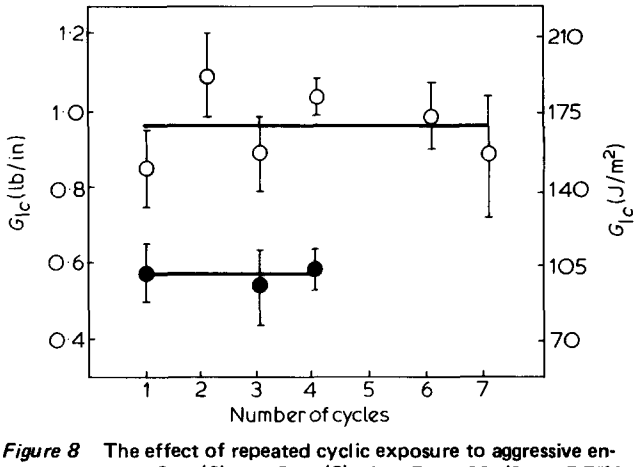

Figure 8 The effect of repeated cyclic exposure to aggressive environment onto G_{Ici} (○) and G_{Ica} (●) of an Epon 825/8 phr DETA system subjected to cure schedule 4 (*Table 3*)

Table 4 Values of the critical strain energy release rate for crack initiation and arrest for an Epon 825/8.4 phr DETA system (formulation 3, *Table 3*), unexposed and exposed to different aggressive environments

Aggressive environment	Bending modulus* E (GPa)	G_{Ici} (J/m²)	G_{Ica} (J/m²)
Laboratory conditions: 72°F + 45% r.h.	2.70	166.25	106.75
Five week immersion in water	1.00	575.75	294.00
Five week immersion in ethyl alcohol	1.05	463.75	229.25

* Value of the bending modulus of the sample cured with 8.4 phr of DETA and exposed to water was extrapolated from *Figure 11*

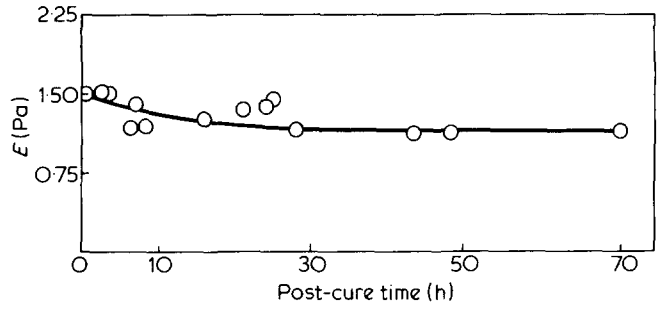

Figure 9 Young's modulus as a function of post-cure time for an Epon 825/8 phr DETA system subjected to cure schedule 1 (*Table 3*)

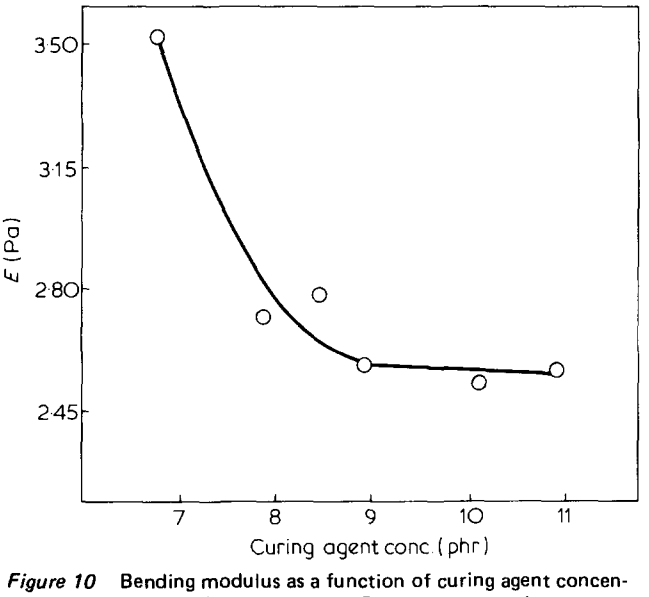

Figure 10 Bending modulus as a function of curing agent concentration for Epon 825/various phr of DETA systems, subjected to cure schedule 2 (*Table 3*)

aggressive environments is offered. The G_{Ic} values for crack initiation seem to be more affected by an aggressive environment. It is worth noting that the most pronounced change in fracture energy occurred upon exposure to water.

Modulus measurements

Values of Young's modulus obtained from the tensile test speciments (Epon 825/8 phr DETA system, cure schedule 1, *Table 3*) were essentially independent of the post-cure time as shown in *Figure 9*. The average value of approximately 1.4×10^9 N/m^2 appears to be low when compared to the values reported in literature[46] (typically 3.5×10^9 N/m^2), and an explanation is offered, at least partly, by considering drawbacks of the experimental procedure. Consequently, somewhat lower tensile modulus values gave rise to higher strain energy release rate values calculated as a function of post-cure time. Tensile modulus values (as a function of post-cure time) were used to calculate *only* the values of fracture energy as a function of post-cure time. Values of bending modulus were used for the calculation of all other fracture energies.

Somewhat surprisingly, experimentally obtained values of bending modulus were found to decrease with increased curing agent concentration as shown in *Figure 10*. An especially abrupt modulus decrease was noticed in approaching the curing agent concentration of approximately 8 phr. Subsequently, a slight decrease of bending modulus values to the stoichiometric concentration of DETA was observed. The beam deflection was monitored with a sensitive *LVDT* device connected to a signal conditioner. Each test was repeated three times with negligible variation between the runs.

Experimentally obtained values of bending modulus of samples exposed to an aggressive environment (liquid water and alcohol) are shown in *Figure 11*. The observed pattern closely resembled that of untreated samples shown in *Figure 10*. An abrupt decrease in modulus to approximately 8 phr of DETA was followed by a slight downward trend. However, it is important to emphasize that the values of bending modulus of treated samples were reduced by a factor of approximately 2.5, when compared with the untreated specimens.

Microscopy

We start this section by presenting electron micrographs from the regions in which a fast crack propagation through the resin took place. Areas of crack initiation and crack arrest, characterized by an apparent plastic flow, are considered later. Several important characteristics of fracture morphology were revealed by a careful examination of micrographs. Fracture proceeded around nodules, indicating that the nodules are the sites of higher crosslink density in the resin. The average size of nodules on all specimens cured with 8 phr of DETA and subjected to cure schedule 1 (*Table 3*) was between 29–32 nm (290–320 Å). Nodular morphology of a typical fracture surface is shown in *Figure 12*. From the corresponding histogram[27], a mean nodule diameter of 30.8 nm (308 Å) was calculated.

Further insight into fracture morphology of bulk epoxy resins was obtained by the use of an etching technique. Etching was done in acetone, in a quiescent bath, at room temperature and for times ranging from 3 h to 8 days. All fracture surfaces were characterized by nodular morphology, as clearly seen in *Figure 13*. Nodules are more pronounced when compared to unetched surfaces, and it appears from the micrograph that the internodular region is preferentially attacked by the etchant. The size of nodules seems to be unchanged by etching. Of considerable interest were the micrographs of etch residues of samples kept in acetone for 8 days. An apparent precipitation of nodules onto microscope slides took place. A presence of resin

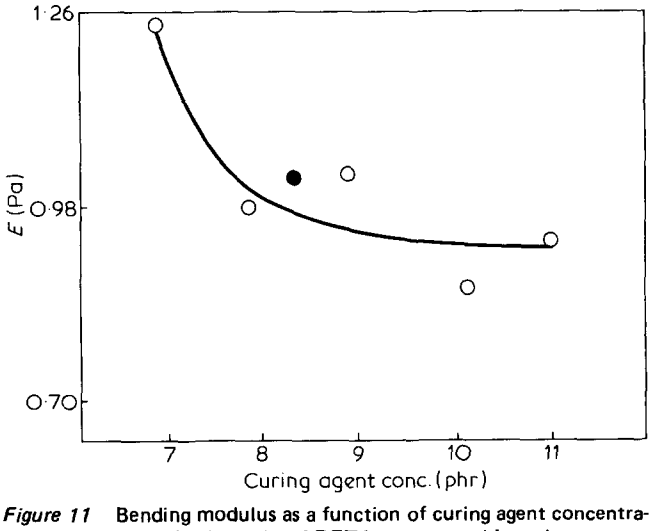

Figure 11 Bending modulus as a function of curing agent concentration for Epon 825/various phr of DETA systems, subjected to cure schedule 2 (*Table 3*). Samples were immersed in either water (○) or ethyl alcohol (●) for 5 weeks

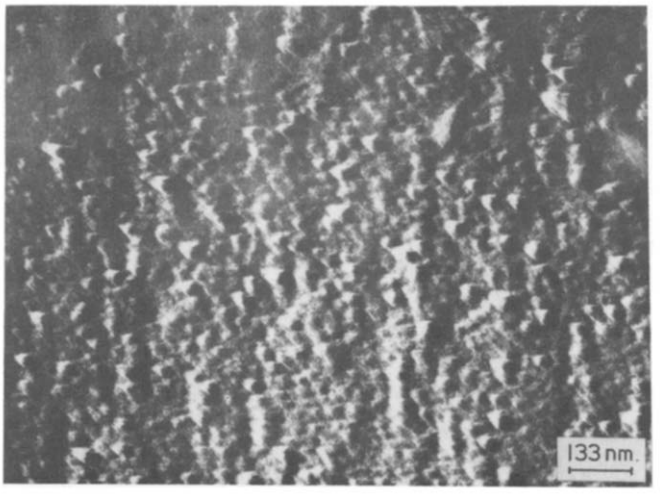

Figure 12 Transmission electron micrograph of a one stage C–Pt replica of fracture surface of an Epon 825/8 phr DETA resin. Sample was cured for 24 h at room temperature and post-cured for 20 h at 106°C. Magnification x 75 000

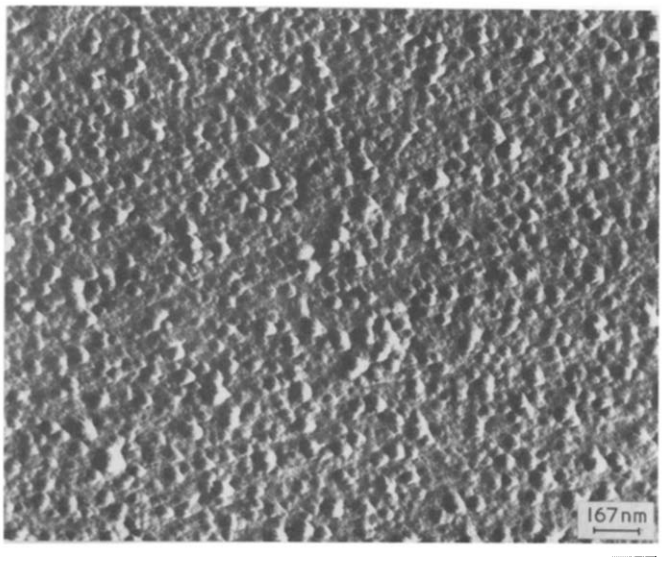

Figure 13 Transmission electron micrograph of a one stage C–Pt replica of fracture surface of an Epon 825/8 phr DETA resin. Sample was subjected to cure schedule 4 (*Table 3*) and cycled for 5 days. Etching was done for 5 h. Magnification x 60 000

chunks, probably due to an incomplete dissolution of internodular matrix, was noted in some cases. These chunks, however, have also displayed a typical nodular character. Etched fracture surfaces of samples cyclically exposed to an aggressive environment (formulation 4, *Table 3*) closely resembled the unexposed samples cured in the same fashion. Some alignment of nodules in the direction of crack propagation was seen, although fine structures 'within' nodules, approximately 1/3 the size of nodules seen previously in electron micrographs[25,26], were not detected.

In order to establish reliability and consistency of the results, replicas were taken at almost every spot along the length and width of the crack propagation plane of different specimens. Variation of the replica location along the width of a specimen was shown to have no effect upon the appearance of nodular morphology. Likewise, no dependence of nodular morphology on the replica position along the length of a specimen was noted. Both conclusions are corroborated by persuasive microscope evidence[27]. Electron micrographs of fracture surfaces of numerous samples of various thermal history (post-cure) are shown elsewhere[27]. In addition, the top view of the fracture surface with the replica location and the corresponding nodule size distribution histogram are given for each sample. Interestingly, no significant variation in the size and distribution of nodules with different post-cure times was observed.

The fact that within a given resin formulation nodular size was found to be independent of various post-cure treatments, suggested that nodules probably form prior to gelation and it is only the internodular matrix that is affected by subsequent post-cure treatments. In highly crosslinked thermosets a possibility of extensive intramolecular reactions before gelation has been realized[47]. Clearly if that were the case, we assumed that various epoxy resin/curing agent formulations would produce nodular structures of different size. Having that in mind we prepared a series of resin formulations with curing agent concentrations (formulation 2, *Table 3*), ranging in size from 6.7 phr to the stoichiometric amount of 10.9 phr. As a result, a definite variation in nodular size as a function of curing agent concentration was observed, as shown in *Figure 14*. Nodules ranged in size from approximately 40 nm (400 Å) at 6.7 phr of DETA, to 19 nm (190 Å) at 10.9 phr of DETA. *Figure 15* shows a fracture

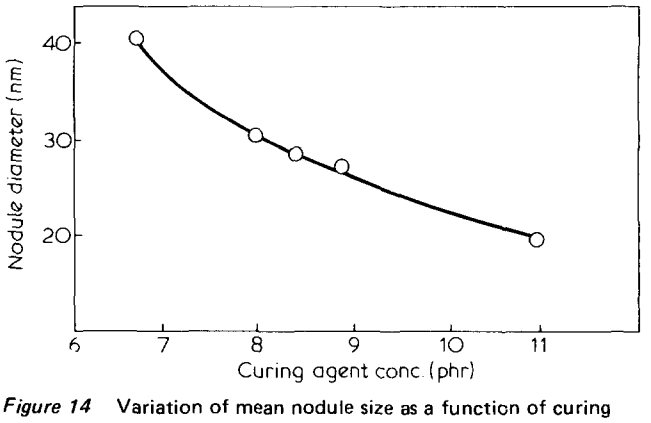

Figure 14 Variation of mean nodule size as a function of curing agent concentration

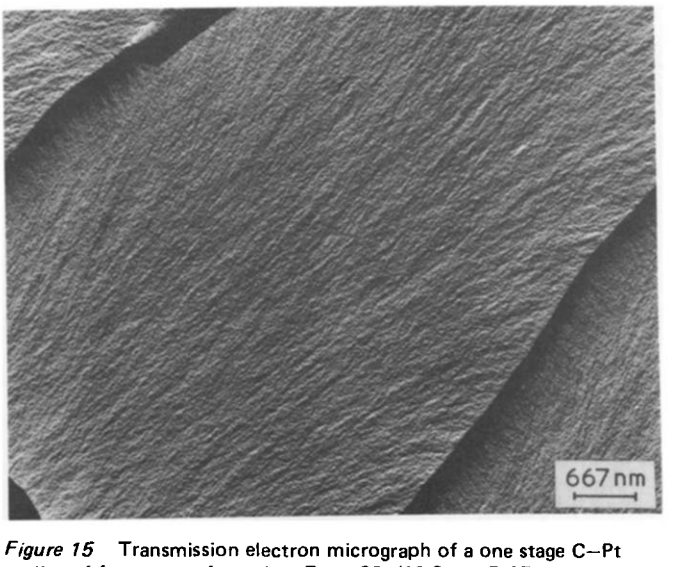

Figure 15 Transmission electron micrograph of a one stage C–Pt replica of fracture surface of an Epon 825/10.9 phr DETA resin. Sample was cured for 20 h at 120°C. Magnification x 15 000

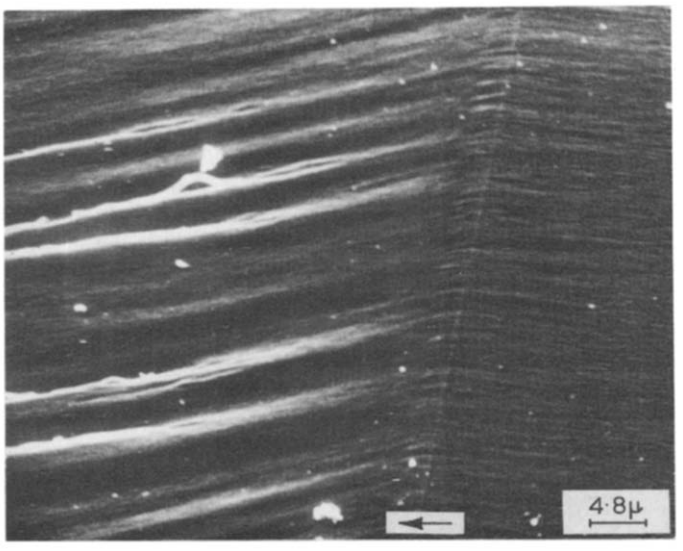

Figure 16 Scanning electron micrograph of fracture surface of an Epon 825/8 phr DETA resin. Sample was cured for 24 h at room temperature and post-cured for 3 h at 106°C. The crack initiation and arrest regions are clearly visible. Magnification x 2100

surface of sample cured with 10.9 phr DETA with an average nodule diameter of approximately 19 nm.

A typical *SEM* micrograph of crack arrest and crack initiation regions is shown in *Figure 16*. To the right of the crack arrest area, a crack propagates in an elastic manner through the region typified by nodular morphology described above. No significant plastic flow was detected in that area due to the high crack speed. Eventually, as the crack speed changes (typical for the strain rate sensitive materials), an increased inelastic deformation causes the local crack extension force to drop below the critical value of strain energy release rate, at which point the crack arrests. The crack front at arrest, previously described[48] as 'fingernail', has a parabolic shape with the leading edge of the crack propagation front in the middle of the beam. Upon reapplication of the load, crack initiation occurs at many points along the width of the beam. The reinitiation starts slowly with cracks often reinitiating in a plane different from that in which they had arrested. Large amounts of plastic flow are indicated by a considerable surface roughness. The initiation marks (steps or ridges) are visible to the naked eye. A step-like appearance characterizes initiation regions and the 'flow' of material towards the edge of a step can clearly be seen. Nevertheless, the plastic deformation region is confined to a relatively small length of approximately several hundred μm. Beyond that point the critical value of strain energy release rate is reduced and fast crack propagation, characterized by a mirror-smooth appearance to the naked eye, takes place.

Interestingly, at both crack initiation and arrest positions, a thorough investigation of upper and lower beams indicated tearing ridges on the upper beam corresponding to ridges on the lower beams. This observation is in agreement with findings of Patrick[48] who maintains that the upper beam is a mirror-image rather than a male–female fit of the lower beam at the arrest site.

From the scanning electron microscope studies we were not able to deduce correlations between the size and appearance of the plastic zone at specimens post-cured for different times and with various curing agent concentrations. A more elaborate picture of the morphology of crack initiation and arrest areas has been obtained from the transmission electron microscopy.

The evidence from *TEM* studies also indicates, in agreement with scanning electron microscopy, that a crack initiates at many points along the width of the crack propagation plane. The initiation stage is characterized by a slow crack propagation, as judged by considerable material 'flow' during an apparent step formation. Energy dissipated in this plastic (inelastic) flow contributes to the calculated G_{Ic} value. When enough energy is supplied to the system and the critical value of strain energy release rate for crack initiation is reached, a step-like fracture occurs along the rows of initiation sites (*Figures 17* and *18*). Upon each reinitiation, a crack continued to propagate in a plane different from that in which it had arrested. This observation faithfully parallels the scanning electron microscope evidence. No apparent correlation of periodicity, density and length of steps (ridges) between various specimens was found. Interestingly, the overall appearance of an arrest zone was characterized by numerous ridges, smaller than those of an initiation zone. This effect is clearly seen in both *SEM* (*Figure 16*) and *TEM* (*Figure 17*) micrographs

Careful examination of areas near the steps along which the crack propagation takes place indicates the presence of intact nodules. The size and distribution of nodules in the plastically deformed zone does not vary from the corresponding nodular size and distribution in the 'ideally elastic' fracture zone, for a given sample. Furthermore, no significant deformation of nodules was observed, not even in the proximity of the sharp edge of a step, as shown in *Figure 19*.

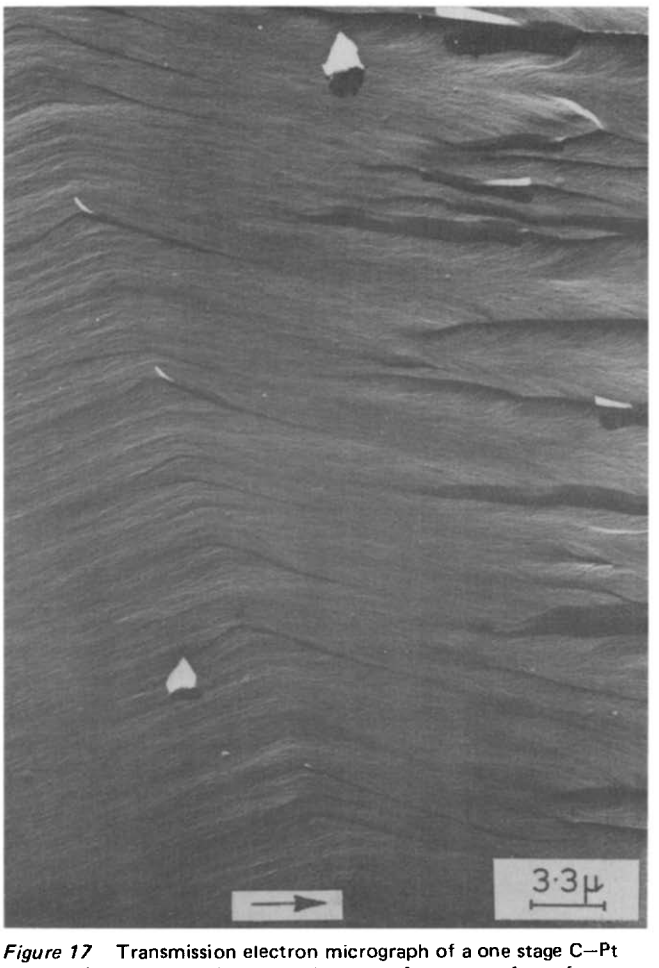

Figure 17 Transmission electron micrograph of a one stage C–Pt replica of initiation and arrest regions on a fracture surface of Epon 825/8 phr DETA resin. Note relatively smooth appearance of the arrest region and numerous steps in the initiation region. The arrow indicates crack propagation direction. Magnification x 3000

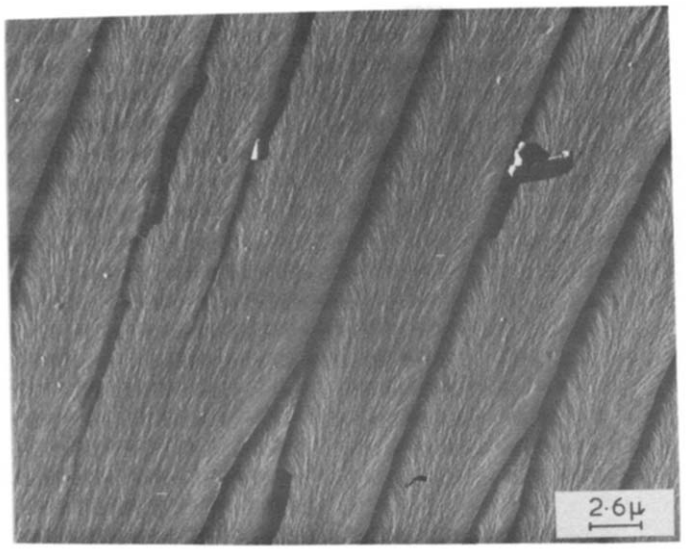

Figure 18 Transmission electron micrograph of a one stage C–Pt replica showing the initiation steps on a fracture surface of Epon 825/8 phr DETA resin. Magnification x 3800

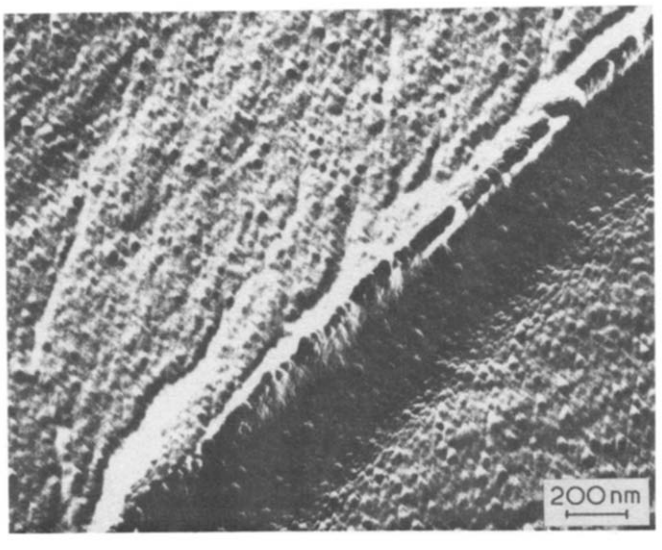

Figure 19 Transmission electron micrograph of a one stage C–Pt replica showing a fracture step in the crack initiation zone of an Epon 825/8 phr DETA resin. Sample was cured for 24 h at room temperature and post-cured for 10 h at 120°C. Magnification x 50 000. A distinct nodular morphology is readily revealed within a step

We further focussed our attention on the nodular structure of the top edge of a step. Needless to say, great difficulties were met in producing C–Pt replicas of initiation region steps and in many cases replicas cracked along the sharp, uppermost edges of a step. Nonetheless, we carefully proceeded to examine the 'splits' in replicas in connection with possible determination of the nature of uppermost nodular layers within a step. Meticulous examinations of many replicas indicated that an intact layer of nodules lies right along the split in each replica. A split apparently occurs in the internodular region between aligned nodules. The electron beam focussed on the split in a replica causes that replica to move, thus making the imaging very difficult.

Finally, in the immediate vicinity of each step a small region, the M–K zone, was defined (*Figure 20*), in which the nodules were being diverted towards the step edge. This zone was measured from the onset of nodular alignment towards the step, to the sharp step edge. Within the M–K zone, no deformation of nodules was observed; it is the 'flow' of surrounding matrix that 'carries' the nodules. A typical *TEM* micrograph showing an initiation region step and the M–K zone of width λ is given in *Figure 21*.

A correlation between the width of M–K zone and the curing agent concentration is shown in *Figure 22*. At lower curing agent concentrations, upon the application of stress, a larger region of lower crosslink density internodular matrix is subjected to 'flow'. As the concentration of curing agent is increased, the brittleness of the matrix increases, resulting in a subsequent decrease in the width of M–K zone. Clearly, λ serves as an indicator of the degree of plastic deformation ir the internodular matrix. Each value of λ is an average value obtained from many *TEM* micrographs by directly measuring the width of the M–K zone. The significance of the M–K zone is further considered in the Discussion section.

DISCUSSION

Although the evidence for the existence of nodules is ample, further support for this idea is offered in the following Discussion. All fracture surfaces investigated during the

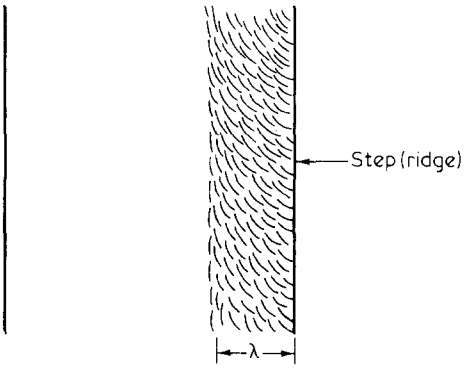

Figure 20 Schematic top view of the M–K zone in which undeformed nodules 'flow' through the plastically deformed internodular matrix

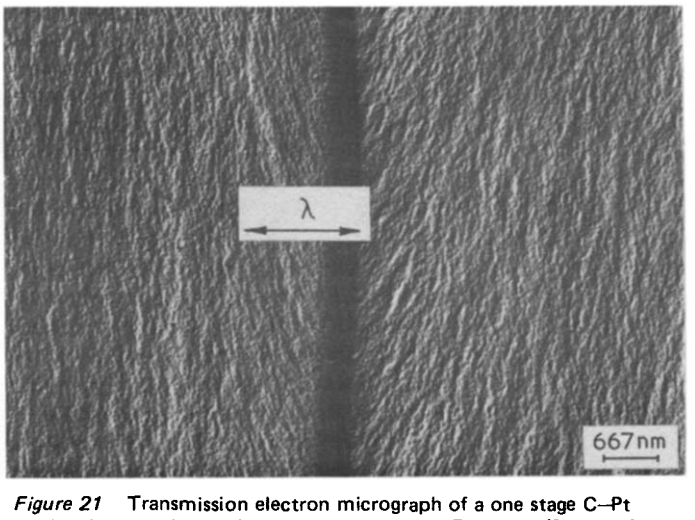

Figure 21 Transmission electron micrograph of a one stage C–Pt replica showing the crack initiation zone of an Epon 825/8 phr DETA resin. Average width of the M–K zone was 1.4 μm. Magnification x 15 000

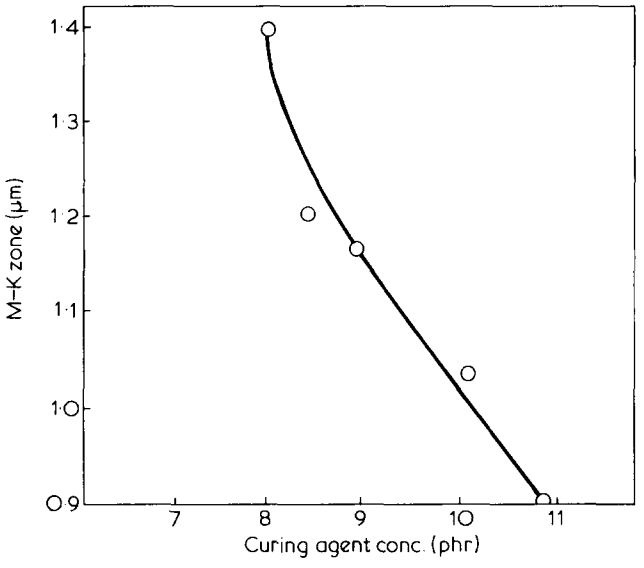

Figure 22 Width of the M–K zone (λ) as a function of curing agent concentration

course of this study were obtained by controlled fracture tests. Consequently, a possibility that the nodular structure is an artefact of the fracture process was considered first and excluded since nodules were observed on the free surfaces of various thermosets as well[26]. That nodules are indeed sites of higher crosslink density has been shown by the fracture proceeding around nodules and by the preferential etching of the internodular matrix and subsequent precipitation of nodules onto microscope slides.

An additional proof for the higher crosslink density nature of nodules emerged from the consideration of formed replica characteristics. Nodules, approximately spherical in shape, were intact during fracture as judged by the shadowing pattern. Immediately behind a distinct nodule, a sharply triangular, platinum-deficient region is formed suggesting a spherical shape.

To exclude the possibility of nodules being an artefact of the replica preparation procedure, other experimental precautions were undertaken. For example, it has been recently suggested that the observed nodular structure in atactic polystyrene (aPS) was an artefact of the C–Pt shadowing technique[49].

Firstly, we would like to emphasize that our work has been concerned with the inhomogeneities in the stucture of brittle thermosetting materials. A considerable amount of research has been carried out concerning the structure–property relationships in brittle thermoplastic materials[50]. Although several theories of the morphology of thermoplastics have appeared, one should bear in mind that the origin and nature of inhomogeneities in the structure of brittle thermoplastics differ from the nodular structure of brittle thermosets. Nevertheless, a possibility of C–Pt shadowing angle-produced artefacts was considered and investigated.

A vast majority of our electron micrographs were of replicas obtained with a Pt bead sitting at an angle of 30° to the specimen surface. Nevertheless, we proceeded to increase the C–Pt shadowing angle up to 90°. Even at approximately 45° angle, blunt replicas of poor contrast were obtained due to a fairly uniform deposition of platinum on the sample surface. Nodules, however, were still detectable; their size and distribution did not change. Therefore, the change of shadowing angle merely affected the contrast and quality of replicas but did not alter the appearance of the structural features. Also, shadowing was performed both in the direction of and perpendicular to the direction of crack propagation without any apparent effect on nodular morphology.

Of considerable interest was the observed alignment of nodules in the direction perpendicular to the crack front. A certain degree of plasticity is expected to exist, especially in a system cured with 8 phr DETA (below the stoichiometric 11 phr). In addition to the crack propagation around nodules in the plane of the advancing crack, dilatational stresses (plane strain conditions) are present in the crack tip region. To relieve these dilatational stresses, which are perpendicular to the crack propagation direction, a movement of nodules through the internodular matrix may occur. This movement, at least in the region away from the crack front, is very small in scale since no step (ridge) formation is observed.

Nonetheless, a controversy still lingers as to the existence of inhomogeneities in brittle thermosets. A repeated failure to detect the nodular structure by SAXS has led these investigators to claim the non-existence of inhomogeneities in thermosets. Recently, Uhlmann[51] suggested that the results of SAXS analysis could explain the existence of inhomogeneities in an epoxy resin provided the density difference between the nodular regions and the matrix is very small (quite unlikely though, according to Uhlmann).

However, an elegant study[46] of density vs. temperature curves for a typical casting epoxy resin showed that the room temperature density difference between the uncured resin (certainly of even lower crosslink density than the matrix) and cured resin was indeed very small (less than 1%). Bearing in mind this small density difference, difficulties encountered in distinguishing the nodular structures from the internodular matrix (e.g. by such methods as SAXS) become apparent.

The initial formation of nodules (although not explicitly studied in this work) probably takes place at numerous random spots in the resin/curing agent mixture. A higher number of nodule formation sites exists in systems with higher curing agent concentration. In these systems, reactive epoxy and amine groups will initiate nodule formation at more sites and consequently smaller nodules will be formed. The internodular material thus obtained is deficient in reactive groups and further crosslinking during post-cure will produce a matrix slightly weaker than that of a post-cured system of lower curing agent concentration (e.g. 8 phr). This behaviour is considered in more detail later in the text to explain the observed drop in modulus with curing agent concentration.

A variation in nodule size is another unambiguous proof for the existence of nodular structures. All investigated replicas were made in identical fashion and consequently the observed variation in nodular size can be accounted for only if nodules are indeed the intrinsic structural features of our systems.

The significance of a curve of the type presented in *Figure 4* is clear when it becomes necessary reliably to assess the brittleness of a material. It is apparent from *Figure 4* (inset) that identical G_{Ic} values are obtained for samples A and B, post-cured for different times. Nevertheless, the brittleness of these samples is different. Although a similar nodular structure has already been established in both samples, the internodular matrix of sample A will undergo further changes upon continuation of post-cure. This observation becomes extremely important when durability predictions are being made. For instance, an assumption that the long-term performance of samples A & B in an aggressive

environment will be identical, may lead to erroneous results. Thus, to avoid possible ambiguities in judgement, we suggest that the critical strain energy release rate be considered a property of brittle materials only beyond a certain maximum value at some post-cure time (corresponding to sample C, *Figure 4*, inset). It is only beyond that point that the decrease in G_{Ic} with post-cure time indeed characterizes the increase in brittleness of materials (G_{Ic} can be thought of as the inverse measure of brittleness). Therefore, we recommend that each study establishing G_{Ic} as an intrinsic property of a given material (at given temperature, loading rate and environmental conditions) should include a G_{Ic} vs. post-cure time dependence.

The difference between fracture energies for crack initiation and crack arrest, designated ΔG_{Ic}, serves as an indicator of the ultimate brittleness of a material under given conditions. The absolute value, ΔG_{Ic}, is not a measure of brittleness in itself; rather, it defines a point (*Z*, *Figure 5*) beyond which the brittleness is not altered by a further continuation of post-cure.

An interesting parallel can be drawn between the G_{Ic} dependence on post-cure time (*Figure 4*) and curing agent concentration (*Figure 6*). It would be misleading to assume that systems A_1 and B_1 in *Figure 6* are characterized by the same degree of brittleness. In fact, only the decrease in G_{Ic} (beyond 8 phr of DETA at the conditions of this study) depicts the actual behaviour of the brittle resins. We maintain that, at the curing agent concentrations of less than 8 phr, our system is not adequately represented by a brittle material constant – G_{Ic}. Two competing effects are to be considered in explaining the initial upward trend of G_{Ic} at low curing agent concentrations (*Figure 6*). Due to the strengthening of resin, an increased energy input is required to deform the material plastically. On the other hand, a simultaneous increase in brittleness is expected to reduce the G_{Ic} value. However, the energy absorbed during the plastic deformation of the resin outweighs the increase in brittleness and consequently an apparent rise in G_{Ic} is seen. The observed subsequent drop in G_{Ic} is caused by the reduced amount of plastic flow, as the brittleness increases further and becomes a predominant factor in determining the ultimate mechanical properties of a resin.

Recalling the observed variation of G_{Ic} with post-cure time (*Figure 4*) and the observation of no apparent change in size and distribution of nodules, we suggest that any dependence of G_{Ic} on the post-cure time should be explained by changes in the internodular matrix[39]. A sudden initial increase in G_{Ic} with post-cure time is attributed to the strengthening of resin (as discussed above) by fast crosslinking of the matrix, and is not adequately represented by a brittle material constant G_{Ic}. This, of course, does not imply the invalidity of the *LEFM* analysis, but simply suggests that the critical strain energy release rate truly 'measures' the brittleness of our resin only beyond the maximum point (C) in *Figure 4*.

In applying the methods of linear elastic fracture mechanics, it is assumed that materials behave 'ideally elastic', i.e. the entire mechanical energy available to the system during the crack growth is spent solely in the formation of new fracture surfaces. In brittle polymers, however, there is evidence that a local plastic flow accompanies the formation of new surfaces and under these conditions, the apparent surface energy may be much greater than the energy of the interatomic bonding[52]. On the other hand, if the region of the inelastic (plastic) response is small compared with the dimensions of the crack, the nature of the stress field and hence the energy associated with it will be negligibly affected[37]. Thus materials are assumed to behave 'ideally elastic', but the apparent value of strain energy release rate will include the energy dissipated in the net inelastic process. Therefore, we next focussed our attention on the discussion of crack initiation and crack arrest regions in an attempt to elucidate the origin and extent of apparent plastic flow.

Two different mechanisms of plastic flow, each absorbing large amounts of mechanical energy, have been identified in glassy polymers[53]. A crazing process has been observed upon tensile yielding and is characterized by molecular orientation and void formation. Most crazing studies are concerned with brittle thermoplastics and are reviewed elsewhere[54]. An interesting interpretation of a failure mechanism of strained epoxy films in terms of a crazing process has recently been offered by Morgan[55]. Voids, approximately 10 nm (100 Å) in diameter, are produced at the craze tip by the tensile dilatational field. Coalescence of small voids results in a formation of larger voids, interconnected by craze fibrils. Within a craze fibril, the epoxy breaks up into intact 6–9 nm particles which are thought to be intramolecularly crosslinked. However, crazing in thick bulk epoxy specimens has not been reported.

Shear banding represents the second mechanism of plastic flow involving molecular orientation over broad, thin curved planes. Unfortunately, there are very few reports on the mechanism of shear banding and no explanation has been offered prior to this work.

Polymer failure by shear banding under given conditions does not imply that the same polymer cannot craze when the applied conditions are changed. Thus, changes in the environmental conditions and specimen geometry (size) can cause a single polymer either to craze or to shear band. Furthermore, even under similar conditions, different polymers may exhibit different plastic flow depending on their internal structure. For instance, Morgan and O'Neal[56] studied a TGDDM/DDS (tetraglycidyl-4,4′-diaminodiphenyl methane epoxy/4,4′-diaminodiphenyl sulphone) system and reported the right-angle steps produced by shear banding. However, only 20% of all their room temperature fractures displayed shear banding. We maintain, as evidenced by our microscopic data, that the step-like fracture pattern is the intrinsic characteristic of crack initiation zones in mode I fracture testing of thick bulk epoxy specimens. The points along which the step formation (shearing) occurs are the loci of high stress concentration and probably correspond either to voids or to the sites of high local concentrations of nodule-deficient, low crosslink density matrix.

Qualitative explanations of the role of higher crosslink density nodules during the various types of network deformation have been offered. For instance, Kreibich and Schmid[23] suggested that one may envision nodules as frozen higher crosslink density segments which act as a framework for the lower crosslink density matrix. An intuitive assumption was made by Gledhill and Kinloch[40], that during plastic deformation of epoxy resins a possible flow of nodules past one another takes place. Unfortunately, no microscopic evidence has been shown. Our micrographs unambiguously disclose the absence of deformation of nodules, thus ascertaining their higher crosslink density (rigidity).

Discovery of the M–K zone enabled us, for the first time, to offer a quantitative correlation of the morphology and ultimate properties of an epoxy resin. *Figures 23–25* represent unique evidence of quantitative correlations between the fundamental morphology (as characterized by both fast and slow crack propagation zones) and ultimate mechanical

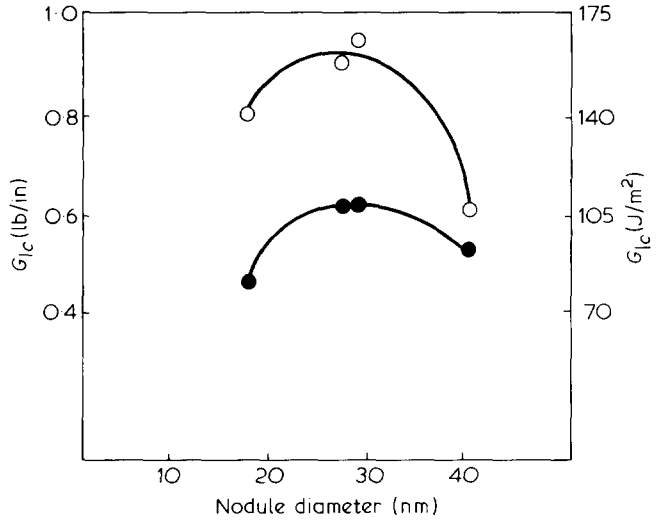

Figure 23 Correlation between the nodule size and the critical strain energy release rate for an Epon 825/DETA bulk system. ○, G_{Ici}; ●, G_{Ica}

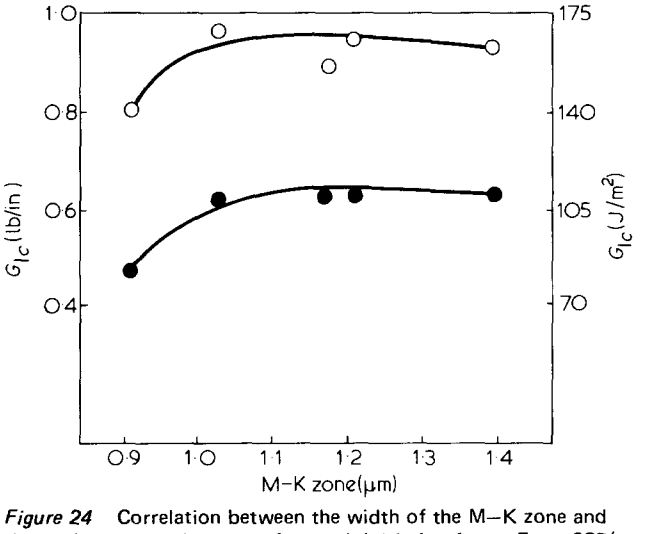

Figure 24 Correlation between the width of the M–K zone and the strain energy release rate for crack initiation for an Epon 825/DETA bulk system. ○, G_{Ici}; ●, G_{Ica}

properties (as characterized by critical strain energy release rate values) of DGEBA/DETA-type epoxy resins.

A somewhat surprising decrease in bending modulus with increased curing agent concentration led us to undertake a careful literature search from which several reports on decrease in modulus with increasing curing agent concentration resulted[17,18,35,46]. Kenyon and Nielsen[17] measured dynamic mechanical properties of an epoxy resin (DGEBA/TETA) and found that, at room temperature, lower shear modulus was obtained at higher curing agent concentration. They accounted for the lower modulus of amine-rich formulation (resin to curing agent ratio of 6:1) by suggesting an inhomogeneous (two-phase) epoxy system composed of higher modulus particles embedded in a lower modulus matrix, with the modulus of the cured resin being determined by the modulus of the matrix phase. The resin rich (resin to curing agent ratio 9:1), one-phase system was assumed to be homogeneous, although no microscopic evidence was given. While we tend to agree with the proposed two-phase system (for the amine-rich formulation), it is questionable whether the system rich in resin would have the assumed homogeneous characteristics.

Several factors should be considered to account for the decrease in modulus with increased curing agent concentration in thermosetting resins. If nodules indeed form prior to gelation, as suggested by several authors[7,12,13] it is likely that unreacted curing agent and epoxy groups would preferentially react in their immediate vicinity (due to conformational and rotational barriers to diffusion). That an extensive intranodular crosslinking is a consequence of conformational barriers has recently been proposed by Chompff[47]. Labana *et al.*[18] presented a statistical argument that the probability of intramolecular reactions within 'gel balls' (nodules) exceeds that of the internodular reactions, leading to the formation of low crosslink density matrix. Assuming that the formation of nodules commences at random spots in the resin-curing agent mixture it is possible that the higher curing agent concentration would lead to excessive intranodular reactions at the expense of a relatively weak matrix. Since the nodules are the sites of higher crosslink density (as clearly shown by microscopic data), mechanical properties of brittle thermosets would be directly determined by the properties of internodular matrix. Therefore, the softening of internodular matrix, as the curing agent concentration is increased, may account for the observed decrease in modulus. This reasoning can also be applied in interpreting Labana's reported drop in tensile modulus values at an amine/epoxy ratio greater than 1:1. On the other hand, had we been able to direct fracture (or bending) through the nodules, higher values of modulus would be expected at higher curing agent concentrations.

Finally it should be mentioned that the manner in which complicated cure chemistry governs the resin morphology is still little understood. For example, Dušek *et al.*[57] have recently shown that the complex chemistry of crosslinking reactions changes as a function of epoxy-to-amine group ratio. Also, a characteristic ribbon morphology was reported[26] in TGEG-type epoxy, indicating a possible presence of linear sequences in these resins. All these facts must not be overlooked when attempting to describe fully changes in mechanical properties caused by variations in curing agent concentrations and cure chemistry, and a clear need for more research efforts in this direction exists.

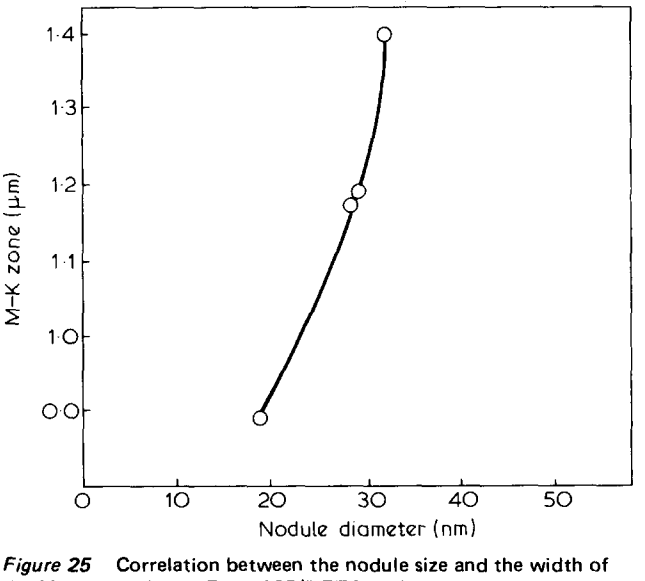

Figure 25 Correlation between the nodule size and the width of the M–K zone for an Epon 825/DETA bulk system

CONCLUSIONS

Various bulk epoxy resin formulations are shown to be characterized by nodular morphology. Much of our data is consistent with the model of higher crosslink density nodules immersed in a lower crosslink density matrix.

A correlation has been established between the morphology of epoxy resins and their ultimate mechanical properties. The size of nodules, as directly determined by various curing agent concentrations, is quantitatively related to the amount of plastic flow in crack initiation and arrest regions. It is suggested that a careful control of cure chemistry can produce a desired morphology, which in turn directly influences the ultimate mechanical properties of a resin. Therefore, the optimization of mechanical properties of bulk epoxy resins can be achieved through a fundamental morphological control.

ACKNOWLEDGEMENTS

The authors wish to thank Dr Sheldon Mostovoy of Materials Research Laboratories in Glenwood, Illinois, whose friendly and effective help was invaluable in initiating the fracture mechanics tests. Special thanks are addressed to the entire Adhesive Research Group of the US Forest Products Laboratory in Madison, Wisconsin, and particularly Mr Bryan River and Mr Arnie Okkonen, who helped with fracture measurements. For the funding of this research we extend our thanks to the Weyerhaueser Company and the US Forest Products Laboratory. Dr C. D. Marshall of the Shell Company in Houston, Texas, supplied large quantities of resin without charge and his contribution is greatly appreciated.

REFERENCES

1 DeBoer, J. H. *Trans. Faraday Soc.* 1936, **32**, 10
2 Smekal, A. 'Handbuch der Physik', Springer, Berlin, 1933, **24** (II)
3 Joffe, A., Orowan, E. and Smekal, A. *Proc. Int. Conf. on Physics, Part, London, 1934*
4 Griffith, A. A. *Phil. Trans. Roy. Soc. London (A)* 1920, **221**, 163
5 Houwink, R. *Trans. Faraday Soc.* 1936, **32**, 132
6 Flory, P. J. 'Principles of Polymer Chemistry', Cornell University Press, Ithaca, New York, 1953
7 Pritchett, E. G. K. *Chem. Ind.* 1949, **2**, 95
8 Megson, N. J. L. 'Phenolic Resin Chemistry', Academic Press, New York, 1958
9 Erath, E. H. and Spurr, R. A. *J. Polym. Sci.* 1959, **35**, 391
10 Erath, E. H. and Robinson, M. *Ibid. (C)* 1960, **3**, 65
11 Wohnsiedler, H. P. *Ibid. (C)* 1960, **3**, 77
12 Bobalek, E. G., Moore, E. R., Levy, S. S. and Lee, C. C. *J. Appl. Polym. Sci.* 1964, **8**, 625
13 Solomon, D. H. and Hopwood, J. J. *Ibid.* 1966, **10**, 1893
14 Solomon, D. H., Loft, B. C. and Swift, J. D. *Ibid.* 1967, **11**, 1593
15 Cuthrell, R. E. *Ibid.* 1968, **12**, 955
16 Kargin, V. A., Pismenko, I. V. and Cherneva, Ye. P. *Vysokomol. Soedin (A)* 1968, **10**, 846
17 Kenyon, A. S. and Nielsen, L. E. *J. Macromol. Sci. (A)* 1969, **3**, 275
18 Labana, S. S., Newman, S. and Chompff, A. J. in 'Polymer Networks', (Eds. A. J. Chompff and S. Newman), Plenum Press, New York, 1971, p 453
19 Kardos, J. L. *Trans.. New York Acad. Sci. II* 1973, **35**, 136
20 Karyakina, M. I., Mogilevich, M. M., Maiorova, N. V. and Udalova, A. V. *Vysokomol. Soedin (A)* 1975, **17**, 537
21 Maiorova, N. V., Mogilevich, M. M., Karyakina, M. I. and Udalova, A. V. *Ibid. (A)* 1975, **17**, 542
22 Morgan, R. J. and O'Neal, J. E. *Polymer–Plastics Technology and Engineering* 1975, **5**, 173
23 Kreibich, T. T. and Schmid, R. *J. Polym. Sci. (Polym. Symp.)* 1975, **53**, 177
24 Racich, J. L. and Koutsky, J. A. *J. Appl. Polym. Sci.* 1976, **20**, 2111
25 Morgan, R. J. and O'Neal, J. E. *Polymer-Plastics Technology and Engineering* 1978, **10**, 49
26 Racich, J. L. 'Boundary Layers in Thermoset Adhesives', *PhD Thesis* University of Wisconsin, Madison (1977)
27 Mijović, J. 'A Correlation Between Morphology and Fracture Properties of Epoxy Resins', *PhD Thesis* University of Wisconsin, Madison (1978)
28 Dušek, K., Pleštil, J., Ledńicky, F. and Luňak, S. *Polymer* 1978, **19**, 393
29 Irwin, G. R. 'Handbuch der Physik', Springer, Berlin, 1958, VI, p 551
30 Ripling, E. J., Mostovoy, S. and Corten, H. T. *J. Adhesion* 1971, **3**, 107
31 Sih, G. C. and Erdogan, F. in 'Linear Fracture Mechanics' (Eds G. C. Sih, R. P. Wei and F. Erdogan) Envo Publishing Lehigh Valley, 1975
32 Ripling, E. J., Mostovoy, S. and Patrick, R. L. *Mater. Res. Stand.* 1964, **64**, 129
33 Broutman, L. J. and McGarry, F. J. *J. Appl. Polym.Sci.* 1965, **9**, 609
34 Obreimoff, J. W. *Proc, Roy. Soc. London (A)* 1930, **127**, 290
35 Mostovoy, S. and Ripling, E. J. *J. Appl. Polym. Sci.* 1966, **10**, 1351
36 Mostovoy, S., Crosley, P. B. and Ripling, E. J. *J. Mater.* 1967, **2**, 661
37 Irwin, G. R. in 'Treatise on Adhesion and Adhesives', (Ed. R. L. Patrick), Vol 1, Marcel Dekker, New York, 1967, p 223
38 Bubsey, R. T., Fisher, D. M., Jones, M. H. and Srawley, J. E. in 'Experimental Techniques in Fracture Mechanics', (Ed. A. S. Kobayashi) Society for Experimental Stress Analysis, Westport, 1973, p 76
39 Mijović, J. and Koutsky, J. A. *J. Appl. Polym. Sci.* 1979, **23**, 1037
40 Gledhill, R. A. and Kinloch, A. J. *Int. Conf. on Fracture Mechanics Techniques, Hong Kong University,* March 1977
41 Gledhill, R. A., Kinloch, A. J., Yamini, S. and Young, R. J. *Polymer* 1978, **19**, 574
42 Bascom, W. D., Cottington, R. L. and Timmons, C. O. *J. Appl. Polym. Sci. (Appl. Polym. Symp.)* 1977, **32**, 165
43 Mostovoy, S. and Ripling, E. J. *J. Appl. Polym.Sci.* 1971, **15**, 641
44 Mostovoy, S. and Ripling, E. J. in 'Adhesion Science and Technology'. (Ed. L. H. Lee), Plenum, New York, Vol 9B, 1976
45 Hertzberg, R. W. 'Deformation and Fracture Mechanics of Engineering Materials', Wiley, New York, 1976
46 Lee, H. and Neville, K. 'Handbook of Epoxy Resins', McGraw–Hill, New York, 1967, p 17
47 Chompff, A. J. *Am. Chem. Soc. Div. Org. Coat. Plast. Chem. Prepr.* 1976, **36**, 529
48 Patrick, R. L. in 'Treatise on Adhesion and Adhesives', (Ed. R. L. Patrick) Vol 3, Marcel Dekker, New York, 1973
49 Thomas, E. L. *presented at the Am. Phys. Soc. Meeting, Washington DC,* March 1978
50 Yeh, G. S. Y. *Pure Appl. Chem.* 1972, **31**, 54
51 Uhlmann, D. R. personal communication
52 Berry, J. P. in 'Fracture Processes in Polymeric Solids', (Ed. B. Rosen), Wiley, New York, 1964
53 Sultan, J. N. and McGarry, F. J. *Polym. Eng. Sci.* 1973, **13**, 29
54 Kambour, R. P. *Macromol. Rev.* 1973, **7**, 1
55 Morgan, R. J. and O'Neal, J. E. *J. Mater. Sci.* 1977, **12**, 1966
56 Morgan, R. J. and O'Neal, J. E. *Am. Chem. Soc. Div. Org. Coat. Plast. Chem. Prepr.* 1977, **37**, 480
57 Dušek, K. and Bleha, M. *J. Polym. Sci.(Polym. Phys. Edn.)* 1977, **15**, 2393
58 Bascom, W. D., Cottington, R. L., Jones, R. L. and Peyser, P., *presented at the Am. Chem. Soc. Meeting, Atlantic City, NJ,* September 1974
59 Diggwa, A. D. S. *Polymer* 1974, **15**, 101
60 Bascom, W. D., Cottington, R. L., Jones, R. L. and Peyser, P. *J. Appl. Polym. Sci.* 1975, **19**, 2545
61 Bascom, W. D. and Cottington, R. L. *J. Adhesion* 1976, **7**, 333